AD-A139 350 APPLICATION OF RAPIDLY SOLIDIFIED SUPERALLOYS(U) PRATT 1/1
AND WHITNEY AIRCRAFT GROUP WEST PALM BEACH FL
A R COX ET AL. NOV 76 PWA-FR-8062 F33615-76-C-5136

UNCLASSIFIED F/G 11/6 NL

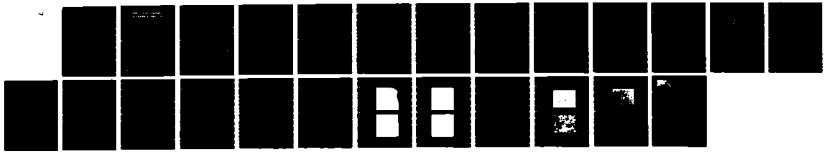

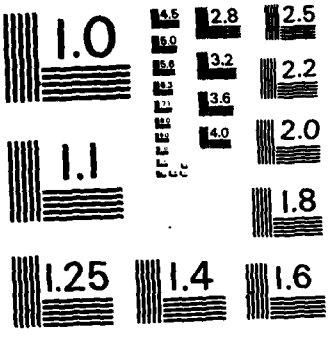

APPLICATION OF RAPIDLY SOLIDIFIED SUPERALLOYS

A. R. Cox
United Technologies Corporation
Pratt & Whitney Aircraft Group
Box 2691, West Palm Beach, Florida 33402

November 1976
Quarterly Report for Period 1 August - 31 October 76

Approved for public release, distribution unlimited.

Sponsored by
Defense Advanced Research Projects Agency

Prepared for
Air Force Materials Laboratories
Wright-Patterson AFB, Ohio 45433

UNCLASSIFIED

SECURITY CLASSIFICATION OF THIS PAGE *(When Data Entered)*

REPORT DOCUMENTATION PAGE	READ INSTRUCTIONS BEFORE COMPLETING FORM
1. REPORT NUMBER	2. GOVT ACCESSION NO. A139350 — 3. RECIPIENT'S CATALOG NUMBER
4. TITLE *(and Subtitle)* APPLICATION OF RAPIDLY SOLIDIFIED SUPERALLOYS	5. TYPE OF REPORT & PERIOD COVERED Quarterly Report 1 August - 31 October 6. PERFORMING ORG. REPORT NUMBER FR-8062
7. AUTHOR(s) A.R. Cox R.J. Patterson	8. CONTRACT OR GRANT NUMBER(s) F33615-76-C-5136
9. PERFORMING ORGANIZATION NAME AND ADDRESS United Technologies Corporation Pratt & Whitney Aircraft Group Box 2691, West Palm Beach, Florida 33402	10. PROGRAM ELEMENT, PROJECT, TASK AREA & WORK UNIT NUMBERS
11. CONTROLLING OFFICE NAME AND ADDRESS Defense Advanced Research Projects Agency 1400 Wilson Boulevard Arlington, Virginia 22209	12. REPORT DATE November 1976 13. NUMBER OF PAGES 22
14. MONITORING AGENCY NAME & ADDRESS*(if different from Controlling Office)* Air Force Materials Laboratories Wright-Patterson AFB, Ohio 45433	15. SECURITY CLASS. *(of this report)* Unclassified 15a. DECLASSIFICATION/DOWNGRADING SCHEDULE

16. DISTRIBUTION STATEMENT *(of this Report)*

Approved for Public Release, Distribution Unlimited

17. DISTRIBUTION STATEMENT *(of the abstract entered in Block 20, if different from Report)*

18. SUPPLEMENTARY NOTES

19. KEY WORDS *(Continue on reverse side if necessary and identify by block number)*

Superalloys, Powder Metallurgy, Rapid Solidification, Turbine Airfoils, Centrifugal Atomization, Convective Cooling

20. ABSTRACT *(Continue on reverse side if necessary and identify by block number)*

This program is being conducted for the purpose of applying the principle of rapid solidification to superalloy powders and subsequent development of stronger compositions for jet engine turbine airfoils. Centrifugal atomization and forced convective cooling of the material are being used for producing the fast cooled material. During this period, characteristics of powder yield resulting from high speed atomization were determined as was actual quench gas requirements on the basis of observed particle size distribution. The yield can be described as a

DD FORM 1 JAN 73 1473 EDITION OF 1 NOV 65 IS OBSOLETE

UNCLASSIFIED

SECURITY CLASSIFICATION OF THIS PAGE *(When Data Entered)*

statistically Normal distribution. The heat release profiles generated by this distribution result in an allowable reduction of about 50% in He gas requirement from original rig design criteria. Eighteen alloy lots were compacted for material evaluations, 14 of which were subsequently extruded. The compaction and extrusion parameters were typical of those used for conventionally processed superalloy powders. Although the results were good visually, recrystallization was not achieved in the manner expected, and it will be necessary to determine effective working procedures specifically for this material.

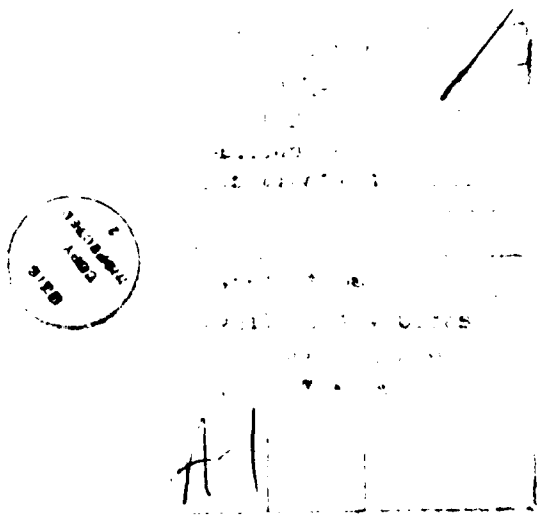

SUMMARY

This program is being conducted for the purpose of applying the principle of rapid solidification to superalloy powders and subsequent development of stronger compositions for jet engine turbine airfoils. Centrifugal atomization and forced convective cooling of the material are being used for producing the fast cooled material. During this period, characteristics of powder yield resulting from high speed atomization were determined as was actual quench gas requirements on the basis of observed particle size distribution. The yield can be described as a statistically Normal distribution. The heat release profiles generated by this distribution result in an allowable reduction of about 50% in He gas requirement from original rig design criteria. Eighteen alloy lots were compacted for material evaluations, 14 of which were subsequently extruded. The compaction and extrusion parameters were typical of those used for conventionally processed superalloy powders. Although the results were good visually, recrystallization was not achieved in the manner expected, and it will be necessary to determine effective working procedures specifically for this material.

CONTENTS

Section		*Page*
I	INTRODUCTION	5
II	PROCESS MECHANICS	6
III	MATERIAL EVALUATION	16

ILLUSTRATIONS

Figure		*Page*
1	Experimental Powder Rig	7
2	Accumulated Wt % vs Particle Size	8
3	95% Confidence Limits on the Population Basis	9
4	Accumulated Wt % vs Particle Size (Modified)	10
5	Influence of Upper Bound on Particle Distribution	11
6	Calculated Particle Heat Release Profiles	12
7	Idealized Cooling Gas Mass Flux Needed to Limit Gas ΔT to 100K	13
8	Effect of Cooling Zone Geometry on Mass Flowrate Requirements	14
9	Mass Flux Requirements for Nine Cooling Zones	14
10	Particle Cooling for Nine Nozzle Configuration	15
11	MAR-M200 Microstructure	17
12	COTAC-3 Microstructure	18
13	Microstructures of HIP and Isothermally Compacted Powders	20
14	Microstructure of MAR-M200 After Extrusion	21

SECTION I

INTRODUCTION

The performance improvements of today's military gas turbine, such as the Pratt & Whitney Aircraft F100, over earlier engines were made possible through advancements in design technology and materials processing. Better alloys, by virtue of chemical composition, played only a minor role in achieving present day capability. Future engine projections, however, are demanding that better materials be developed in order that still higher levels of performance can be achieved.

The turbine module is especially dependent on improvements in such alloy properties as higher temperature capability, better stability, and better corrosion resistance. The alloys presently being used in this section were developed more than 15 years ago. It has not been that a lack of development interest has existed since then that these alloys are still in use. Rather, it has been the inability to improve the nature of alloying under conditions now imposed for subsequent processing and component fabrication. Precision casting alloy compositions are limited because of such constraints as crucible and mold interactions and massive phase occurrence. Forging alloys are limited because of constraints of segregation during ingot processing.

Superalloy powder metallurgy studies conducted at the P&WA/Florida facility have shown that the use of powder, particularly powder solidified at very high rates of cooling, can eliminate the constraints noted and can enable more effective alloying for the improvement of basic material properties. Several examples which support this statement are as follows. Chemical segregation in fast cooled superalloy powders can be controlled to a submicron level. Massive phases can be eliminated. Solubility of alloying elements can be extended without deleterious phase reaction. None of these can be achieved in ingot or precision casting.

Further, the inherent homogeneity of the powder is such that subsequent processing and heat treatment can be used very effectively to promote maximum material utilization. Abnormal grain growth, for example, can be achieved in superalloy powder materials for optimization of mechanical properties above $\frac{1}{2}$ T_M. MAR M-200 alloy powder, processed and reacted in this manner, is, in fact, stronger than, and as ductile as, the same composition cast in a directional mode.

P&WA/Florida has constructed a device that can produce metal powders solidified and cooled at rates in excess of 10^6 °C/sec. The underlying principle is forced convective cooling, whereby powder particles of controlled size are accelerated into a high thermal conductivity gaseous medium maintained at high ΔT between itself and the metal particle.

The purpose of this ARPA sponsored program is to refine the process mechanics used with the powder producing device for fast quenching bulk lots of powder and, subsequently, apply the technology of rapid solidification to the development of an alloy composition that is stronger than the existing MAR M-200 alloy and that can be implemented for the production of better turbine airfoils.

The program is a 40-month effort and is organized as a progression of events starting with a parametric study of the requirements necessary to achieve high yields of fast quenched powder and terminating in the fabrication and testing of turbine airfoils. This report is the third technical report and covers the 7th to 9th month of the program. It deals with the study of producing fast quenched powder and includes observations on resulting material characteristics.

SECTION II

PROCESS MECHANICS

The device used for production of fast cooled powder is one in which a central rotary atomizer disintegrates a molten metal stream into fine particles and accelerates them into a high mass flow helium quench environment. The unit is illustrated in Figure 1 and principal design parameters are based on a metal atomization rate of 0.15 kg/sec. It is presently capable of handling metal charges up to 23 kilograms (based on nickel). The unit has 3 annular gas nozzles which are sized to gas mass flow and velocity commensurate with maintenance of a high ΔT on the basis of calculated heat flux profiles and particle trajectories. For 0.15 kg/sec metal flowrate, the gas requirement translates to ~0.75 kg/sec. A radial impulse turbine is used for the atomizer drive. The unit is provided with conventional vacuum induction melting and tundish metering. The sequence of operations includes vacuum melting, He backfilling, pouring and atomization, and, finally, gas quenching.

In the previous reporting period, the majority of activity was directed toward stabilizing the atomization process at high rotational speeds (21,000 to 24,000 rpm). During that time, the alloy IN100 was used exclusively and it was found that operational stability and high yields of powder could be achieved under conditions where compensation for the varying heat flux on the spinning disk was correctly obtained.

Four major efforts dealing with machine operations were conducted during this report period: (1) Statistical analysis of yield and repeatability of operation, (2) Influence of alloy change on operation and yield, (3) Fabrication of a second generation, higher speed turbine drive assembly, and (4) Evaluation of actual He gas quench requirements on the basis of resulting power size distribution. Fourteen runs were made for the item (1) and (2) purposes. The individual efforts are reported in the following paragraphs.

Three different alloys were used in the 14 runs: IN100 (which had been used previously), Mar M-200, and an experimental cobalt base alloy designated CoTaC-3. The composition of each is listed in Table 1. Changes in densities and fluid properties of these materials which could influence the atomization process appear minor, but are thought to be representative for those of the type alloys to be considered later in the program. The empirical relation for rotary atomization indicates a relationship of the form

$$d = K \left(\frac{\mu^{0.2} \sigma^{0.1}}{\rho^{0.5}} \right)$$

where
- d = particle diameter
- K = constant
- μ = viscosity
- σ = surface tension
- ρ = density

Other than density, physical properties should not significantly affect the atomization yield or particle size distributions. Such was found to be true. In each of the three alloy cases, where machine operating parameters were held constant, the yield and characteristics thereof were essentially the same.

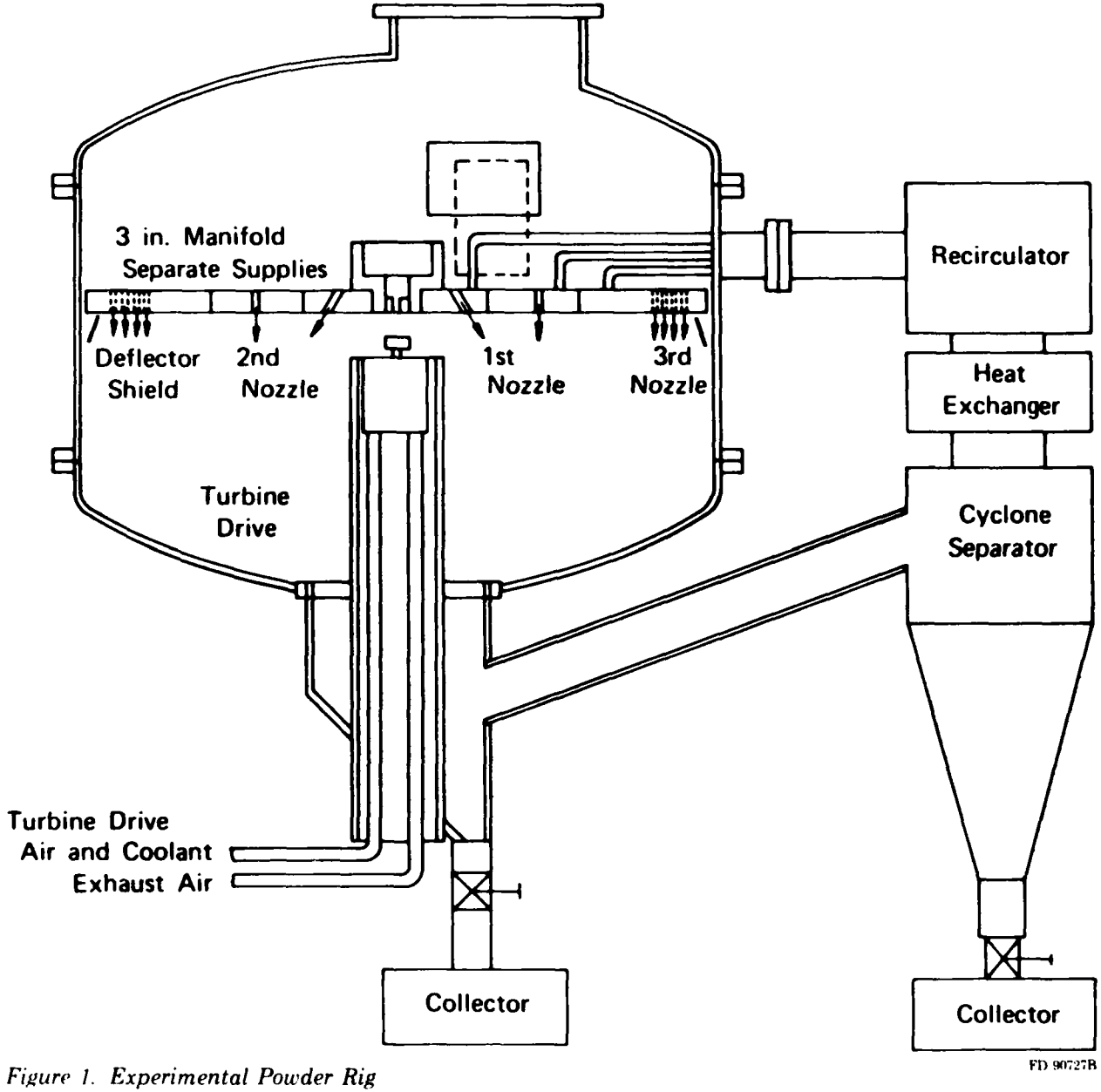

Figure 1. Experimental Powder Rig

TABLE 1. ALLOY COMPOSITIONS

	IN100	*MAR M-200*	*CoTaC-3*
Ni	BAL	BAL	10.0
Co	18.0	9.5	BAL
Cr	12.5	9.0	19.3
Al	4.8	5.0	-
Ti	4.5	2.0	-
Mo	3.5	-	-
W	-	12.0	-
Ta	-	-	13.0
B	0.015	0.015	-
C	0.06	0.15	0.7
Zr	0.06	0.04	-
V	0.7	-	-
Cb	-	1.0	-

Note: Numbers indicate nominal weight percent

To statistically analyze yield, 12 runs were made at 24,000 rpm (equivalent to ~100 m/sec). All machine parameters with respect to metal flowrate, superheat, quench, etc., were held constant and were those previously reported for operation. A flat surface was used for half the runs and a concave form for the balance. The concave shape was selected as an alternate form since numerous reports of rotary atomization indicate higher efficiencies with curved surfaces. The behavior of the mean distribution for each set, based on −10 mesh (2000μm) = 100%, is shown in Figure 2. Figure 3 depicts the limits, with 95% certainty, for the two means.

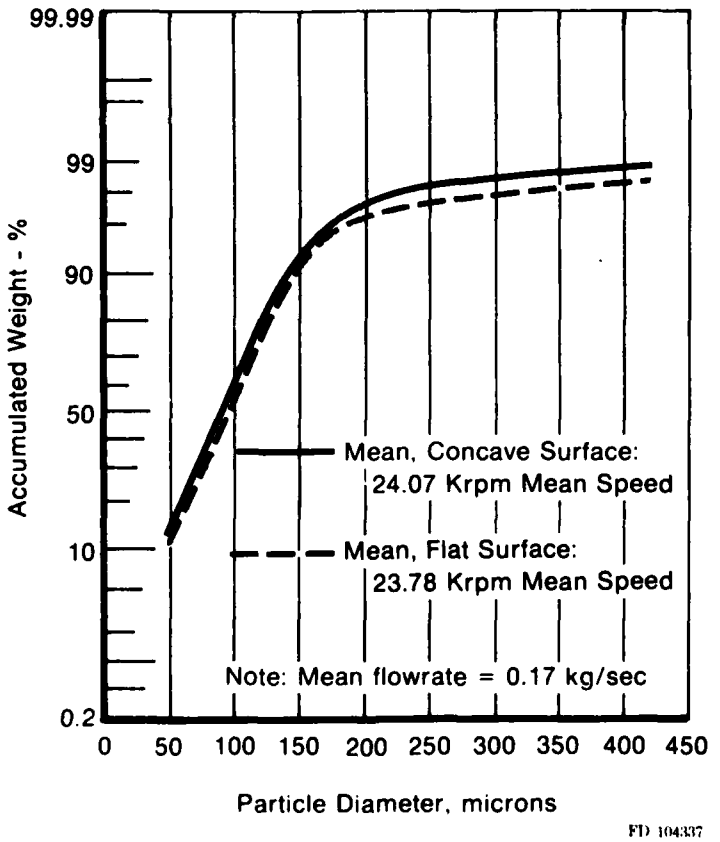

Figure 2. Accumulated Wt % vs Particle Size

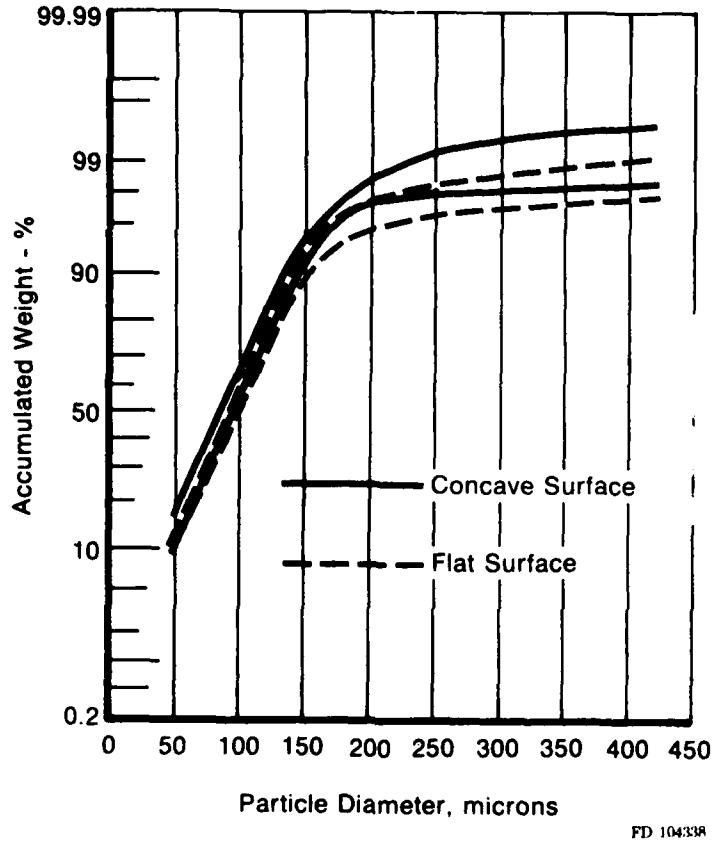

Figure 3. 95% Confidence Limits on the Population Basis

Figure 4 depicts a "statistical trick" used to check linearity and the data to a model; in this case, the Normal distribution. The probability scale of the paper used is generated from tabulated values of an integral of the form

$$P(z) \propto \int_{-\infty}^{z} \exp(-z^2/2)\, dz$$

In this integral, z is a reduced variable of the form

$$z = (x-\mu)/\sigma$$

where μ has been set equal to zero and σ has been set equal to 1. In the general case, however, it may be found that the data contain the parameters μ and σ. In this case, a graph of the data on probability paper can be linearized by adopting arbitrary values for these parameters until the "best fit," or most nearly straight line, is achieved.

As can be seen from the figure, the mean distribution for the concave disk is linearized for a displacement of about 2.5 wt %. The extrapolation at the low end of the graph was based on values taken from a plot of the data on log-probability paper, on which values below 45 microns will be substantially lower than would occur on Normal probability paper.

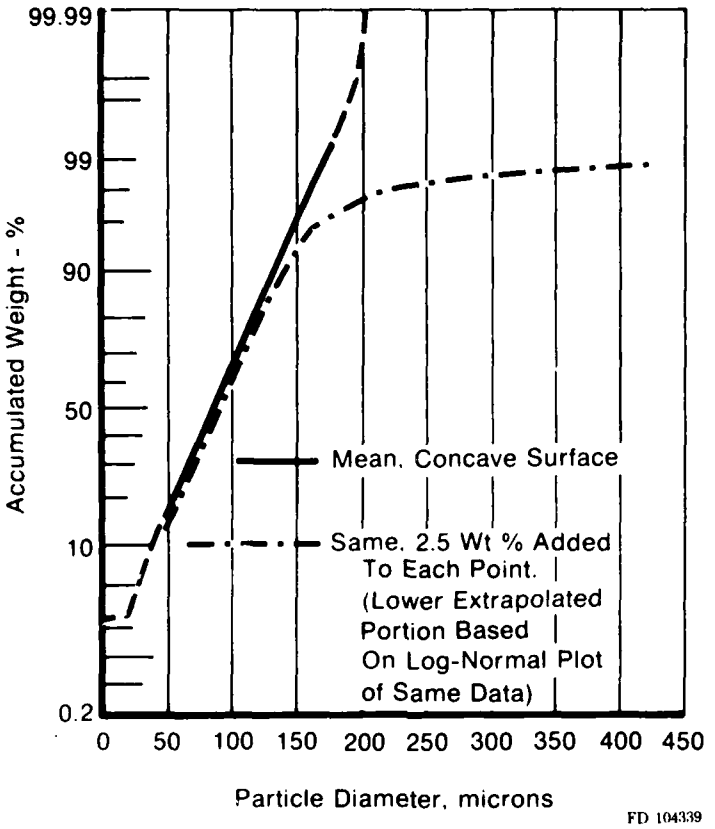

Figure 4. Accumulated Wt % vs Particle Size (Modified)

While the improved linearity might be due to the presence, in the data, of a location parameter μ having a value near 2.5 wt %, we feel that other sources of nonlinearity can be the presence of a skewed distribution and the inclusion of more than one distribution in the data plotted.

As noted in our second report, it is not unreasonable to assume that material produced during the start of a run might display a distribution different from that obtained for the majority of the run occurring after initial transients. Too, distributions which are right-skewed can be linearized by proper plotting on log-probability paper while our distributions in general become even more nonlinear on such paper.

These considerations suggest that while a location parameter might be the cause of the nonlinearity, a more probable source might be the presence of two (or more) distributions. Figure 5 shows such a circumstance. Selected here was one of the runs used in obtaining the mean curve shown in Figure 4. The graph of the data based on -10 mesh = 100 wt % is the third curve from the top. If the material above 60 mesh is simply ommitted, so that normalization becomes -60 mesh = 100 wt %, the second curve from the top is obtained.

The rapid nonlinear rise seen above about 175 microns can be due to the fact that pertinent data above this point have not been included. Another source, however, is the presence of material which is not made by the process responsible for the distribution below 175 microns.

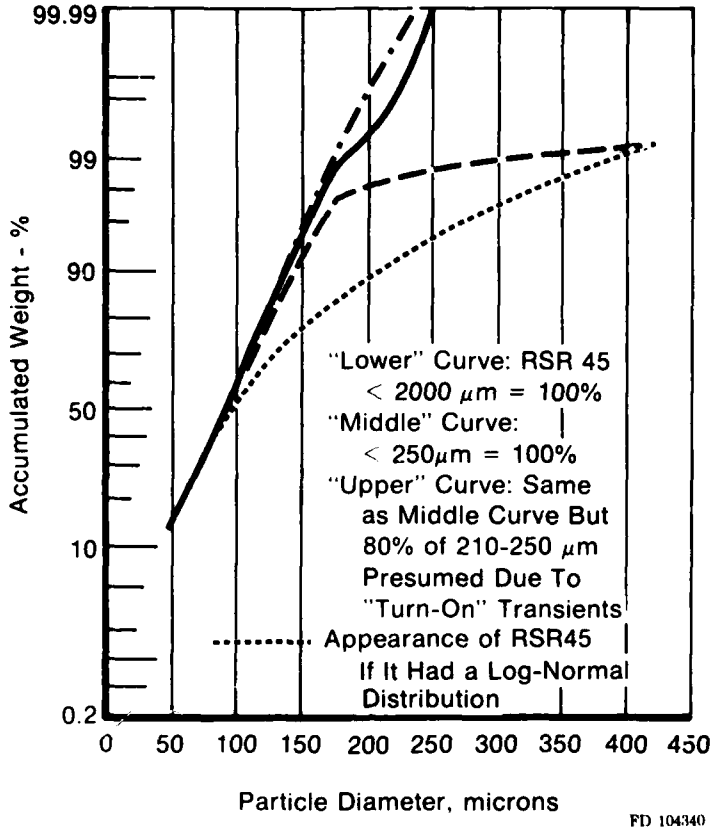

Figure 5. Influence of Upper Bound on Particle Distribution

Because the hypothesis is that material above 60 mesh is made by a process different from that producing the bulk of the material below 60 mesh, it is not unreasonable to extend the hypothesis and presume that a small portion of the material in the range −60+80 is also due to the process operating above 60 mesh. If one simply presumes that for this particular run, about 80% of the −60+70 material is really due to the mechanism resulting in the +60 material, then the result is the uppermost of the four curves plotted. As can be seen, the hypotheses result in a very good fit to the Normal model; too, the result is that the mean particle size, based on weight, has been shifted downward by about 5 microns.

The lowest curve on the figure displays the shape that the run would have produced had the log-Normal model been applicable. This curve was obtained by using the points from the data normalized to 10 mesh, at 75 and 45 microns, on log-probability paper. Extending the curve to 40 mesh and replotting the extrapolated data back onto Normal probability paper results in a log-Normal "run" plotted on Normal paper, and shows the general shape we might expect to see if our runs were log-Normal rather than Normal.

How far below 45 microns the distribution remains Normal cannot now be conveyed. However, we are aware that we cannot expect the 1 to 2 wt % at zero microns which extrapolation of present curves would indicate. In general, the curve is expected to fall off at 10 or 15 microns. In this region, the cyclone separator starts to become ineffective, and the powder seems to become more adherent to such surfaces as chamber walls, collectors, and separator, as well as to the sieves and possibly also to other powder particles. Thus, our data below 10 to 15 microns is likely to be censored by the system. Even if enough material is produced to provide a linear Normal behavior down to this range, the material is not likely to be observed, and by 10 microns at least, the curves will start to fall off toward zero wt % faster than the Normal model would predict.

The new turbine drive assembly, which will produce twice the tangential speed and atomization studies up to 200 m/sec, is not yet operational. Therefore, little more, if any, is known now about rotational speed dependence on particle size and distribution than was known in July. All components for the new assembly have been fabricated, but, because it is necessary to progressively balance the unit as it is assembled, more time has been required than thought originally. It is expected that this new unit will be operational by the end of the year.

The original analysis of He quench requirements was based on an exclusive generation of 50μm particles with subsequent heat release, relative to location, velocity, etc., based soley on criteria associated with this particle size. Now that it is possible to identify a size distribution, the computer-aided cooling rate and gas mass and velocity profile studies initially used to size the device were iterated to re-evaluate quench and nozzle conditions on the basis of observed atomization.

The technique was used to calculate heat flux as a function of distance from the atomizer for the particle size range typified in Figure 3. The resultant profile is shown in Figure 6 and is in the form of an envelope which accounts not only for variation in particle velocity but also for variations in gas velocity and inlet gas temperature.

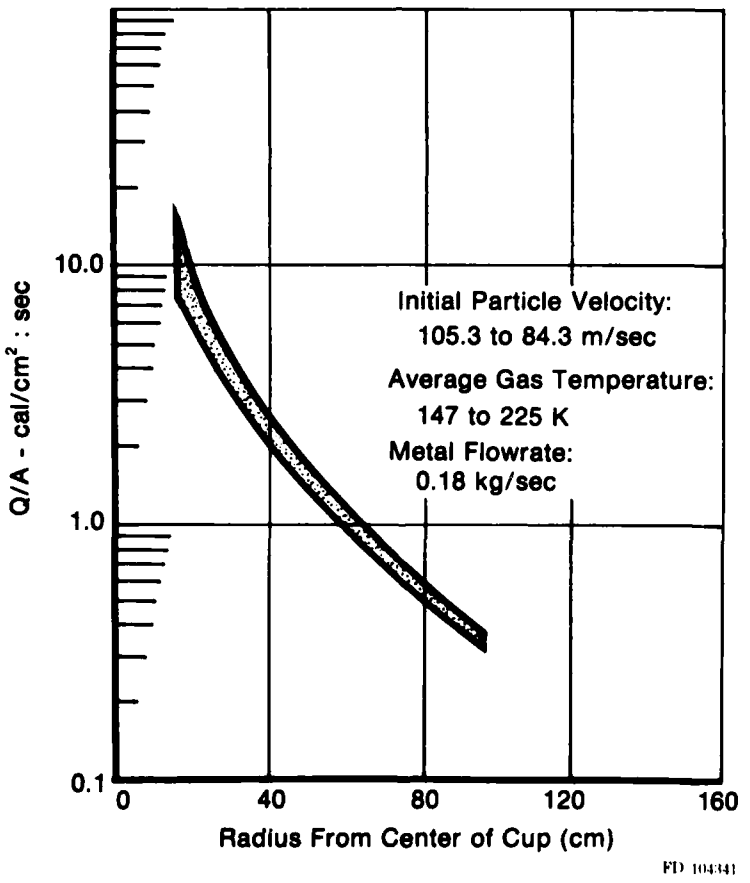

Figure 6. Calculated Particle Heat Release Profiles

Based on this profile, a gas mass flux requirement was calculated and is shown in Figure 7. Used in these calculations were an inlet gas temperature of 230°K, an acceptable gas temperature rise of 110°K, a metal flowrate of 0.18 Kg/sec, and an initial particle velocity of about 100 m/sec.

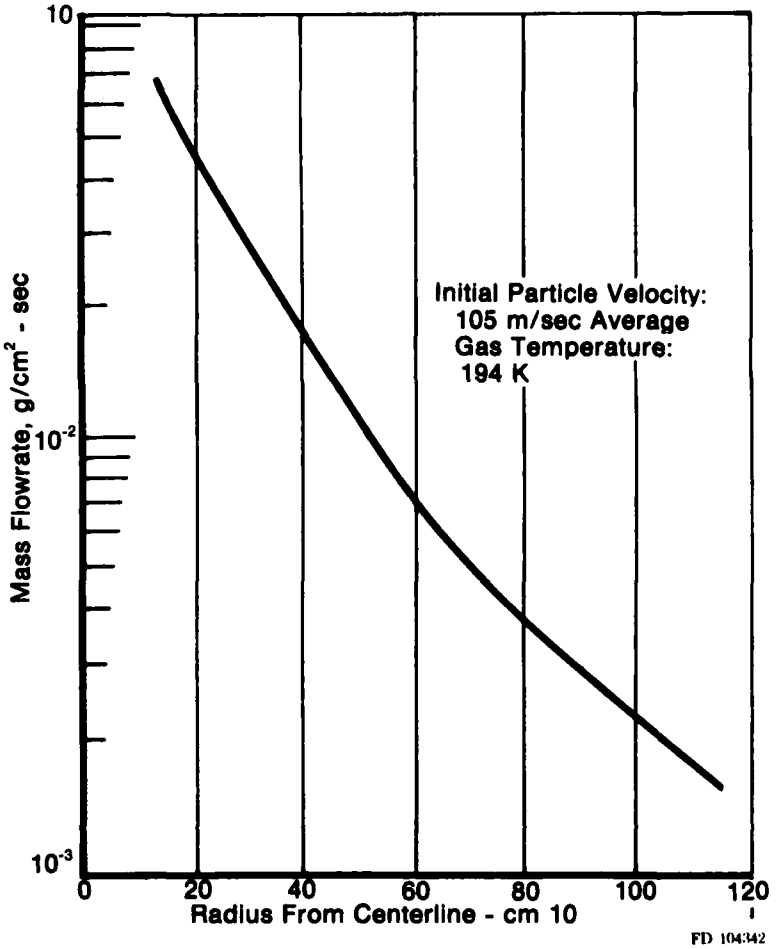

Figure 7. Idealized Cooling Gas Mass Flux Needed to Limit Gas ΔT to 100K

Nozzle requirements for both cross-flow and swirl are being evaluated with respect to the data depicted in Figure 7. The cross-flow analysis is complete and the results are discussed subsequently.

For cross-flow quenching, an infinitely variable nozzle is the ultimate solution to compensate for the continuously changing heat flux. Since it is impractical, however, the effect of simulating such a nozzle with a finite number of nozzles was investigated, with a basis that each would have uniform and independent flowrates. The total gas mass flowrate required to limit the gas temperature increase of 110°K or less at any point on a zone was calculated as a function of the number of equally spaced annular zones. The results are shown in Figure 8. As can be seen, as the number of zones increases, the total flowrate decreases. Nine zones appear practical; in both number and total flowrate required, and the percentage of gas mass flowrate per zone is shown in Figure 9. Presuming that the particle density does not inhibit gas flow and particle cooling in the zones nearest the origin, this configuration requires only about 0.39 Kg/sec He to accommodate the heat release shown in Figure 6. Resultant particle cooling under these circumstances is shown in Figure 10 and is essentially the same as that described in our first report.

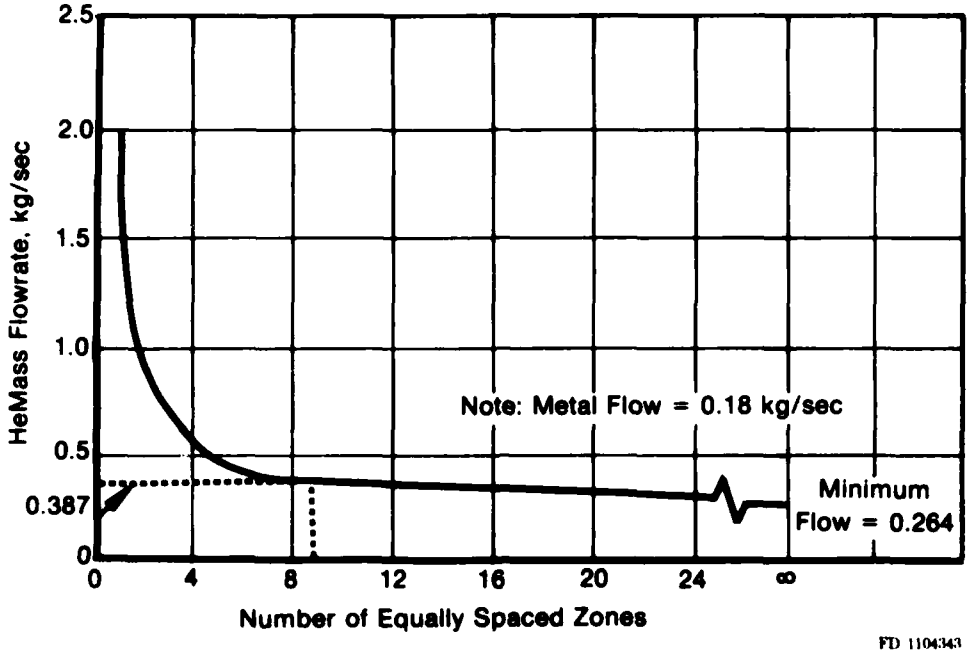

Figure 8. Effect of Cooling Zone Geometry on Mass Flowrate Requirements

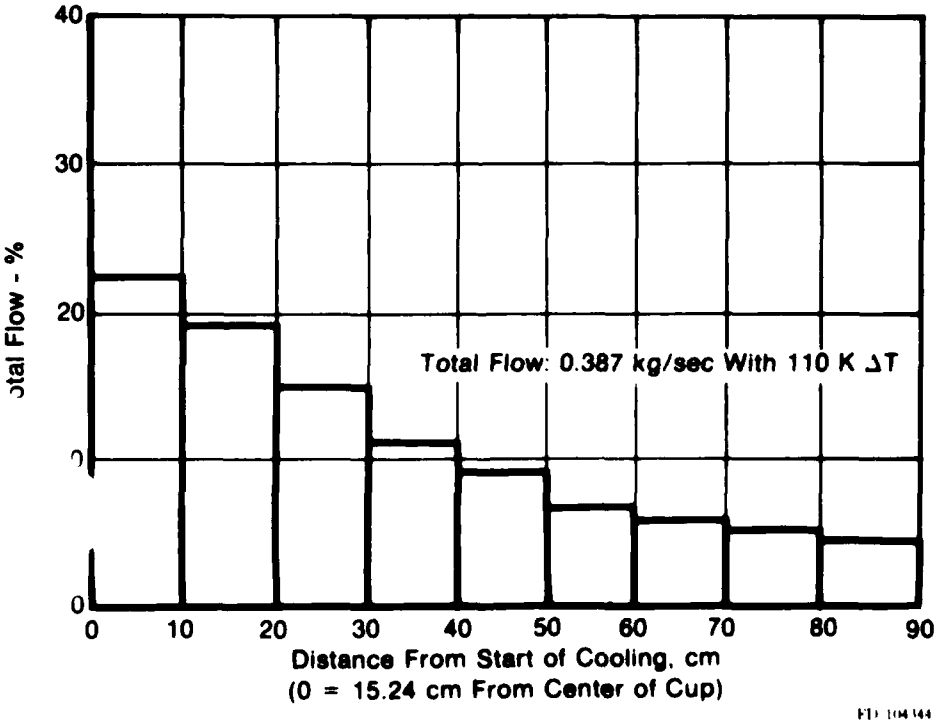

Figure 9. Mass Flux Requirements for Nine Cooling Zones

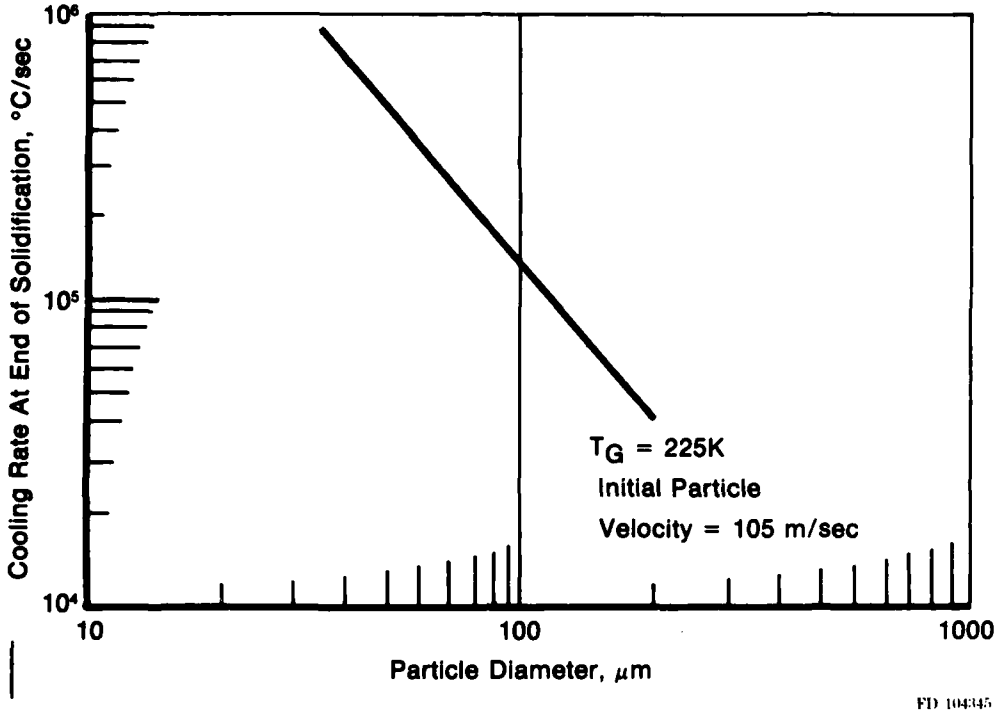

Figure 10. Particle Cooling for Nine Nozzle Configuration

These data suggest that the present requirement of gas mass flow can be reduced by about 50% for the particle distribution presently being obtained. The swirl flow analysis will be completed during the next report period and, once the new turbine drive is installed and a final analysis of particle distribution and yield can be obtained, an overall assessment of true gas requirements can be determined.

SECTION III

MATERIAL EVALUATION

Analyses of the powder from each lot have been performed in the manner reported previously. Observations continue to show attainment of rapid solidification and suppression of secondary phases.

The typical microstructure of MAR M-200 alloy powder is shown in Figure 11, that of CoTac-3 is shown in Figure 12. Both alloys show a significantly reduced concentration of precipitated carbide (the principal strengthener in the CoTac-3 material). The MAR M-200 material further shows no precipitation of the γ' phase, its principal strengthener. Both alloys exhibit homogeneity on the same scale as described in previous reports.

It was noted in the previous report that a "microcrystalline" structure, different from the dendritic form, could be produced in IN100 alloy powders, especially in the very fine particles. This remained true with the MAR M-200 alloy as well.

The CoTac-3 alloy was generally dendritic but it was made on a single setup and it could well be that different operating parameters could likewise have produced the other form. Both the dendritic and microcrystalline forms of MAR M-200 are shown in Figure 11. As with the IN100 alloy, greater homogeneity was obtained in the latter structure.

We had hoped to relate the structural differences to superheat extraction during the atomization but our efforts during this period were inconclusive for this purpose. There is growing belief, however, that the fine grain material is the result of a rheocasting type phenomenon, rather than an undercooling circumstance, which was our initial impression. If the rheocast circumstance is the case, dendrites would be nucleating on the atomizer surfaces, breaking apart, and being swept with residual liquid metal into the quench media. Proof of this condition is necessary, but it is an interesting conjecture and could lead to important studies in other areas of material development.

Scanning transmission election microscopy appears to be the best aid to continue the study of the microcrystalline form. Preparation of powder samples for this purpose is difficult and, to date, we have had no success in the area. University researchers, however, have reported that they have developed the means to produce the necessary sample shapes. Hopefully, therefore, results of microchemical differences should be available within the next several months.

Consolidation and working procedures for the powder materials were started during this period. Tooling for isothermal compaction was constructed and procedures for powder outgassing and sealing established. In addition to the four IN100 extrusions made in the previous period, four additional lots of IN100 were extruded, four lots of IN100 hot isostatically compacted, and ten lots of MAR M-200 extruded. With minor exceptions, the methods of compaction and reduction were the same as those used for conventional superalloy powder materials. Table 2 lists the entire series of operations.

The powder lots used for consolidation were maintained under inert conditions during all operations. Outgassing prior to containerization was done at a rate of about 0.4 Kg/min at 315°C and $\sim 10^{-4}$ Torr, using a pump speed of about 3000 l/sec (based on He). The isothermal compactions were run in TZM Molybdenum potting dies using a uniaxial load, HIP in a standard HIP press, and conventional compaction in a blanked-off extrusion press.

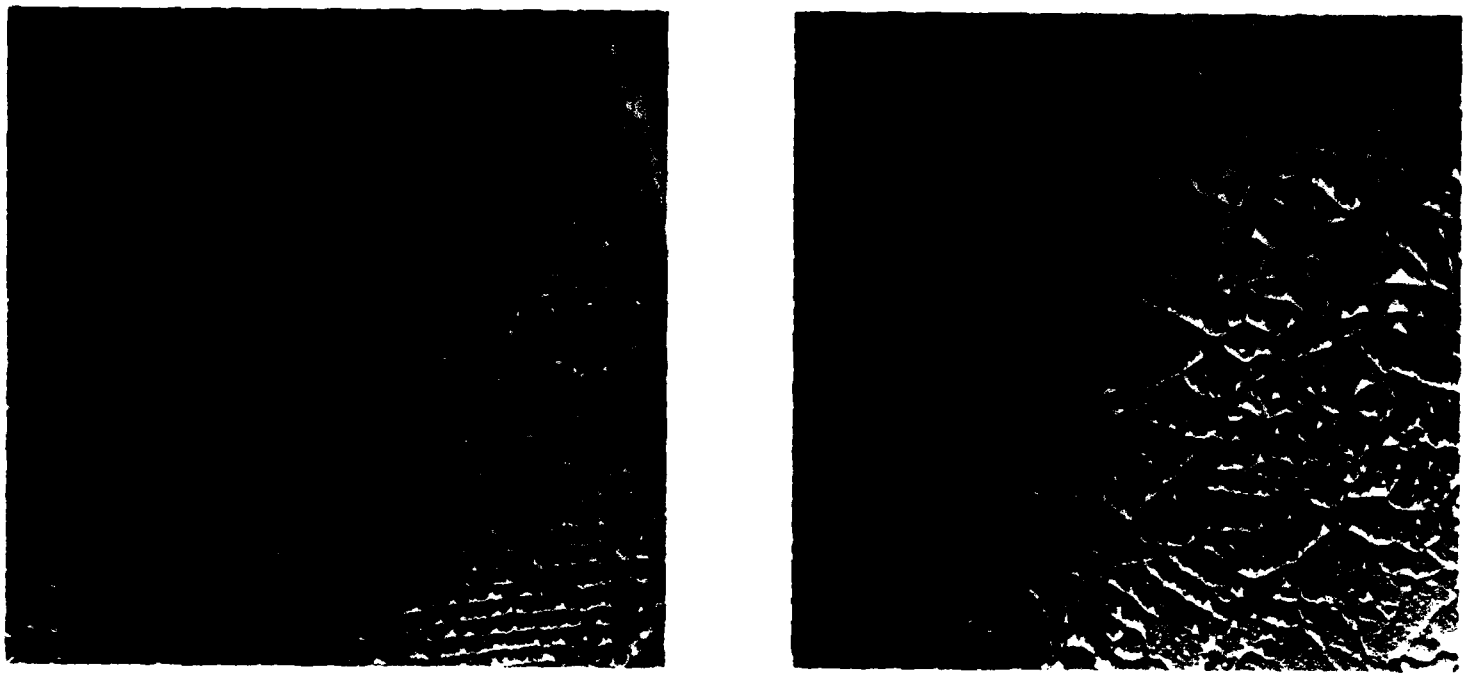

Mag: 3000X

Particle Size ≤ 105 μm

FD 1104346

Figure 11. MAR-M200 Microstructure

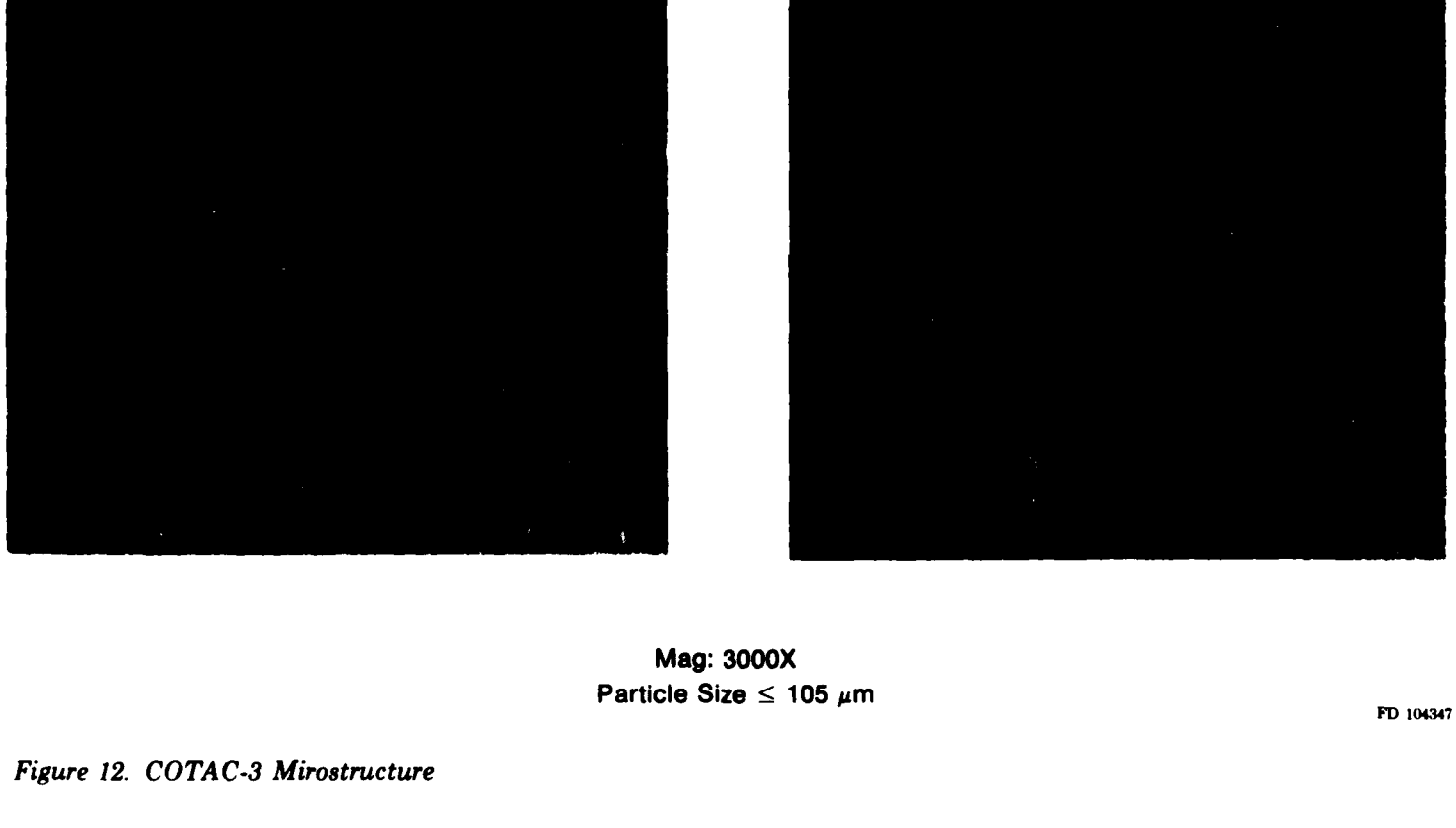

Mag: 3000X
Particle Size ≤ 105 μm

FD 104347

Figure 12. COTAC-3 Mirostructure

TABLE 2. CONSOLIDATION/EXTRUSION OPERATIONS

		Compaction			Extrusion	
Alloy/ID	*Type*	*Temp(°C)*	*Pressure, Pa×10⁸*	Time(hr)	Temp(°C)	Reduction
IN100-23	Isothermal	1010	2.07	4	1065	~6/1
IN100-25	Isothermal	1010	2.07	4	1065	~6/1
IN100-26	Isothermal	1010	2.07	4	1065	~6/1
IN100-27	Isothermal	1010	2.07	4	1065	~6/1
IN100-37	HIP	1218	1.03	8	-	-
IN100-39	HIP	1218	1.03	8	-	-
IN100 40	HIP	1218	1.03	8	-	-
IN100-42H	HIP	1218	1.03	8	-	-
IN100-36	Conventional	1010	13.03	0.017	1065	~6/1
IN100-42	Conventional	1010	13.03	0.017	1065	~6/1
IN100-43	Conventional	1010	13.03	0.017	1065	~6/1
IN100-44	Conventional	1010	13.03	0.017	1065	~6/1
MAR M-200-45	Isothermal	1010	1.37	4	1121	~6/1
MAR M-200-47	Isothermal	1010	1.37	4	1121	~6/1
MAR M-200-49	Conventional	1093	13.03	0.017	1121	~6/1
MAR M-200-50	Conventional	1093	13.03	0.017	1121	~6/1
MAR M-200-51	Conventional	1093	13.03	0.017	1065	~6/1
MAR M-200-54-1	Conventional	1093	13.03	0.017	1121	~6/1
MAR M-200-54-2	Conventional	1093	13.03	0.017	1121	~6/1
MAR M-200-55-2	Conventional	1093	13.03	0.017	1065	~6/1
MAR M-200-55-3	Conventional	1093	13.03	0.017	1121	~6/1
MAR M-200-55-4	Conventional	1093	13.03	0.017	1121	~6/1

Both the isothermal and HIP compactions resulted in essentially 100% density. Neither, however, resulted in bulk recrystallization. Typical microstructures are shown in Figure 13. The photomicrograph of isothermal compaction is fairly representative of results of both IN100 and MAR M-200. The compacted form resulting from conventional consolidation was not evaluated directly but, from observation of the extruded material, particle bonding and densification were not achieved for the selected condition.

With the exception of the two MAR M-200 extrusions run at 1065°C, all barstock was visually sound. The two at 1065°C ruptured during reduction. However, with the exception of the material which had been isothermally compacted, all barstock exhibited internal defects of the type normally associated with too cold an operation and/or insufficient work. Recrystallization remained incomplete for all cases. Typical microstructures are shown in Figure 14. For the case of isothermal compaction, recrystallization after extrusion was about 75% complete. For conventionally compacted material, recrystallization was only about 50% complete. Oxygen levels were low on all barstock, averaging between 35 and 80 ppm, and was not considered to be a contributing factor to the unbonded condition. Samples from the material which had been isothermally compacted and extruded were forged into simple round configurations with no problems, but afterward, the previously unrecrystallized areas remained unrecrystallized. These results were not expected since these same working parameters have been used successfully with conventional gas atomized superalloy powders. No specific reasons for the observed differences are given at this time.

The heat-treat effort is based primarily on achieving abnormal grain growth and only in isolated instances was this achieved. The barstock, therefore, has been rejected on the basis of improper work parameters and a second set of material lots is being prepared to study varying temperatures and reduction on recrystallization and subsequent grain growth.

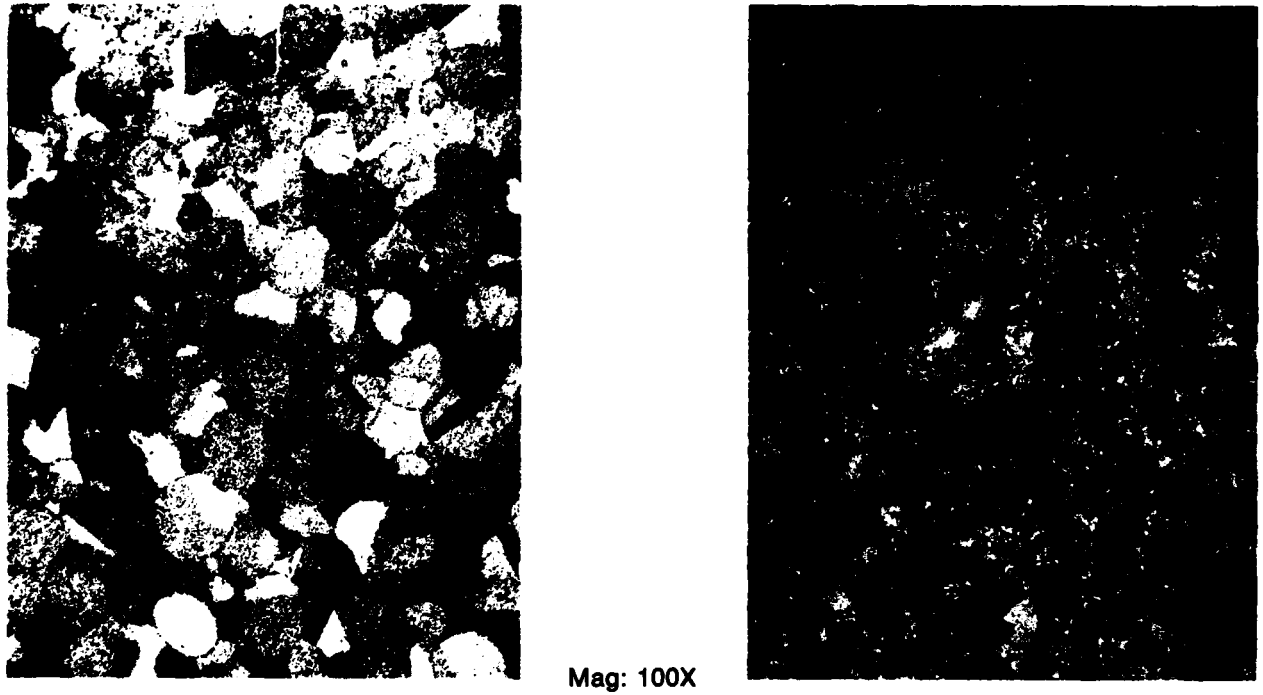

Figure 13. Microstructures of HIP and Isothermally Compacted Powders

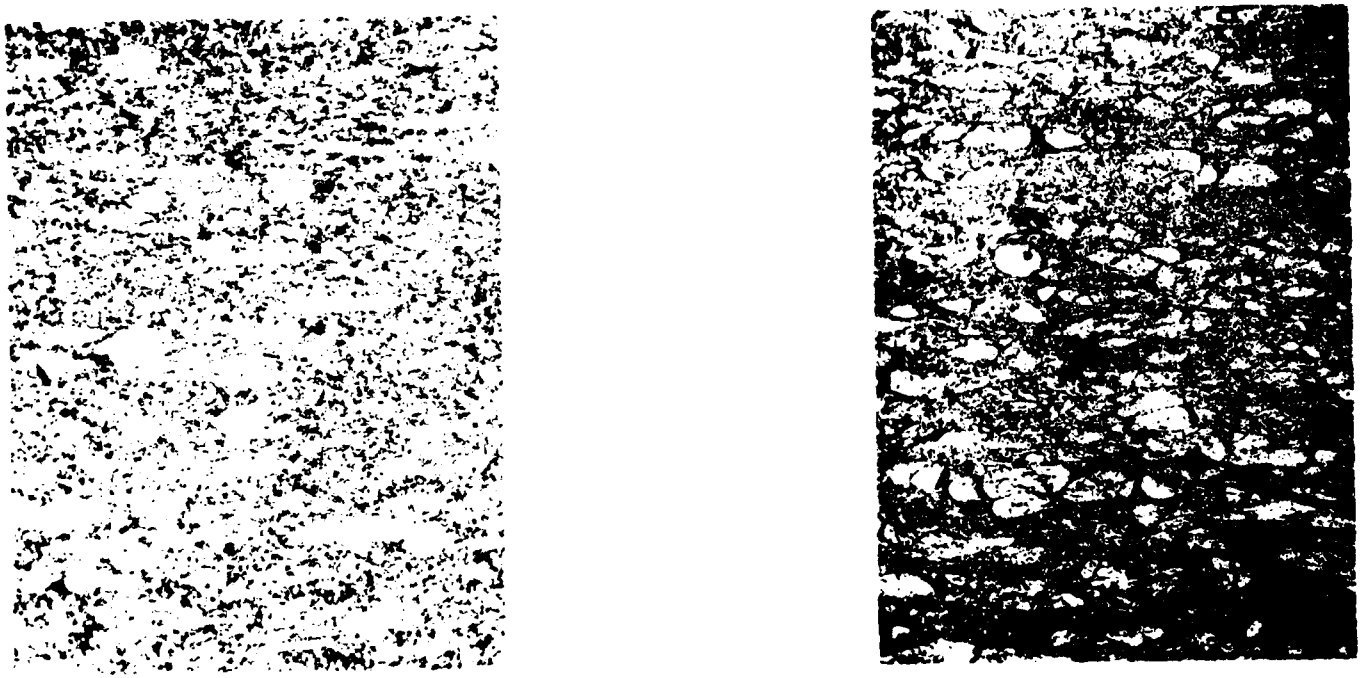

Isothermally Compacted
S/N 45

Mag: 100X

Conventionally Compacted
S/N 55-4

FD 104349

Figure 14. Microstructure of MAR-M200 After Extrusion